Valence-band parameters and g factors of cubic zinc selenide derived from free-exciton magnetoreflectance

H. Venghaus
Max-Planck-Institut für Festkörperforschung, 7 Stuttgart 80, Federal Republic of Germany
(Received 6 September 1978)

Reflectance spectra were measured on cubic ZnSe crystals in magnetic fields up to 18 T and transverse energies of the $1s$-exciton states derived by a line-shape fit. The results are analyzed combining the existing low-field theory of Γ_6-Γ_8 exciton states with the results of variational calculations for excitons in polar materials without valence-band degeneracy. The observed linear Zeeman splitting yields a conduction-band electron g factor $g_c = 1.37 \pm 0.25$, an effective hole g factor $\tilde{\kappa} = -0.21 \pm 0.06$, corresponding to $\kappa = -0.28 \pm 0.08$, and an upper limit for the short-range electron-hole spin exchange $2\Delta_1 \lesssim 0.1$ meV. From the $1s$-$2s$ exciton-state energy separation we derive the exciton Rydberg $R_0^* = 16.8 \pm 0.4$ meV and obtain $E_{1s} = 17.4 \pm 0.4$ meV exciton binding energy. The observed diamagnetic-shift rates yield an exciton reduced mass $\mu_0^*/m_0 = 0.095 \pm 0.003$ corresponding to $\gamma_1^* = 4.3 \pm 0.5$ for $m_e^*/m_0 = 0.16$. We further determine $\gamma_2^* = 0.59 \pm 0.07$ and $\gamma_3^* = 1.34 \pm 0.30$. The bare valence-band parameters γ_i derived from the renormalized parameters γ_i^* are $\gamma_1 = 4.8 \pm 0.6$, $\gamma_2 = 0.67 \pm 0.08$, and $\gamma_3 = 1.53 \pm 0.35$. With the parameters derived, energy shifts and splittings of exciton states not used for the evaluation of the parameters are calculated in good agreement with the experimental results. The exciton reduced mass derived from diamagnetic-shift rates yields an exciton Rydberg in good agreement with the Rydberg obtained from the $1s$-$2s$ exciton-state energy separation. Finally, the energy separations of $2p$-exciton states calculated from our parameters are in close agreement with two-photon absorption measurements. This is taken as a justification for the theoretical model applied and suggests the derivation of fundamental parameters of related compounds such as CdTe or ZnTe along similar lines.

I. INTRODUCTION

Magneto-optical experiments on exciton states in semiconductors provide a means to determine fundamental parameters such as electron and hole g factor, exciton reduced mass, electron-hole spin-exchange energy or valence-band parameters γ_i.[1-3] An analysis of the shift and splitting of the substates emerging from the $1s$ exciton ground state, which is eightfold degenerate in a zinc-blende type semiconductor like cubic ZnSe, yields the parameters required, provided an adequate theoretical model exists.

In the present paper we report magnetoreflectance measurements on cubic ZnSe in magnetic fields up to 18 T. 18 T corresponds to $\gamma \simeq 0.6$ [cf. Eq. (3.12g)], and accordingly the application of existing low-field theories[1,2] is possible only after appropriate modifications, and further corrections are required, since ZnSe is a highly polar material.

For the analysis of our experimental data we choose a combination of the low-field Γ_6-Γ_8-exciton theory[2] with a variational calculation according to Behnke *et al.*[4] assuming: (i) all parameters entering the expressions in Ref. 2 are regarded as renormalized parameters; (ii) diamagnetic terms are reduced in the same way as calculated in the corresponding two-band model according to Ref. 4; and (iii) the linear Zeeman terms remain unchanged.

Since the theoretical analysis is based on transverse eigenenergies, these are derived from the experimental reflectance curves by means of a line-shape fit.[5] The exciton-photon interaction (polariton effect) is taken into account as it is generally done and Feierabend and Weber[6] are in error with their recently raised objection with respect to a similar analysis already published.[7]

The paper will be organized as follows: Experimental details are outlined in Sec. II. Section III starts with a compilation of formulas necessary for the line-shape analysis. Then the important results representing the Γ_6-Γ_8-exciton ground state in low magnetic fields[2] are summarized. At the end of Sec. III corrections for polar materials such as ZnSe are presented, which are not restricted to the limit $\gamma \ll 1$. Experimental results are given in Sec. IV, beginning with the electron and hole effective g factor and an upper limit for the short-range electron-hole spin-exchange energy. Then we derive the exciton Rydberg, the exciton reduced mass, and a set of valence-band parameters γ_i. In Sec. V the present results are compared to theoretical and experi-

mental data of other authors. Finally, excited exciton states and their interpretation are presented in Sec. VI.

II. EXPERIMENTAL

The experiments were performed both on polished (100) and cleaved (110) surfaces of not intentionally doped cubic ZnSe crystals, grown from the melt. After mechanically polishing, the (100) faces were treated with the modified form of Ichimiya's etch[8] as given in Ref. 9. The crystals were mounted strain free in a helium flow exchange gas cryostat and cooled down to ~4 K. Reflectance was measured with a quartz-iodine or xenon lamp and a conventional optical system. The detection system consisted of a $\frac{3}{4}$-m single grating monochromator, a photomultiplier tube and a lock-in amplifier. The magnetic field was produced by a 12-T superconducting magnet or alternatively by a 10-MW 20-T Bitter-type magnet.

III. THEORY

A. Line-shape analysis

Our analysis of the magnetic field induced energy shifts and splittings of the exciton ground state subcomponents will be based on Ref. 2. All energies are given in terms of transverse exciton states, and consequently these have to be derived from the magnetoreflectance spectra, while an analysis based on the relative separation of reflectance minima leads to incorrect results. In the present investigation the transverse eigenenergies are derived from the reflectance spectra by means of a line-shape fit. According to Ref. 5 theoretical reflectance curves are calculated from a dielectric function with two resonances including spatial dispersion:

$$\epsilon(\omega, k) = \epsilon_b + \sum_{j=1}^{2} \frac{4\pi\beta_j \omega_j^2}{\omega_j^2 - \omega^2 + k^2\hbar\omega_j/M_j - i\omega\Gamma_j}, \tag{3.1}$$

where $4\pi\beta_j$ is the strength of the jth oscillator, M_j is the translational exciton mass to be calculated as described in Refs. 10 and 11, and Γ_j is an empirical damping constant.

The wave vectors k_i (or refractive indices $n_i = k_i c/\omega$, $i = 1, 2, 3$) corresponding to the three transverse modes propagating in the crystal are obtained from Eq. (3.1) by the condition $\epsilon(\omega, k) = k^2c^2/\omega^2$, giving an equation cubic in k^2. Without exciton free layer the amplitudes of the three bulk modes E_1, E_2, and E_3 and that of the reflected wave E_R can be calculated from the following set of equations:

$$n_0 E_I - n_0 E_R = n_1 E_1 + n_2 E_2 + n_3 E_3, \tag{3.2}$$

$$E_I + E_R = E_1 + E_2 + E_3, \tag{3.3}$$

$$\sum_{k=1}^{3} c_k^j E_k = 0, \quad (j = 1, 2), \tag{3.4}$$

where

$$c_k^j = \frac{1}{\omega_j^2 - \omega^2 + b_j n_k^2 \omega^2/c^2 - i\omega\Gamma_j}, \tag{3.5}$$

$$b_j = \hbar\omega_j/M_j. \tag{3.6}$$

E_I is the amplitude of the incoming wave and n_0 is the refractive index of the medium outside the crystal (e.g., air). Eqs. (3.2) and (3.3) represent the well-known Maxwell boundary conditions, while the additional boundary conditions (3.4) correspond to the requirement, that the contribution from each resonance to the polarization must vanish at the sample surface.[12-14]

The effect of an exciton free layer of thickness D and characterized by a background polarizability $\epsilon_b = n_b^2 = k_b^2 c^2/\omega^2$ is taken into account defining an effective refractive index n_{eff} of the bulk crystal

$$n_{\text{eff}} = \frac{n_1 + n_2 E_2/E_1 + n_3 E_3/E_1}{1 + E_2/E_1 + E_3/E_1} \tag{3.7}$$

and then the formula given in Ref. 15 for reflectance on a multilayer system yields

$$R = \left| \frac{E_R}{E_I} \right|^2 = \left| \frac{(n_b - n_0)(n_{\text{eff}} + n_b) + (n_b + n_0)(n_{\text{eff}} - n_b)\exp(i2k_b D)}{(n_b + n_0)(n_{\text{eff}} + n_b) + (n_b - n_0)(n_{\text{eff}} - n_b)\exp(i2k_b D)} \right|^2. \tag{3.8}$$

The agreement between experimental and theoretical reflectance curves can be improved further assuming a damping $\Gamma_i(r)$, which depends on the distance r to the sample surface and smoothens the change of the optical properties from the exciton free surface region to the bulk.[16]

We did not apply this refinement, since there was no need to do so for our present purposes.

B. Exciton shift and splitting

The conduction-band electron and the hole g factor, g_c and $\tilde{\kappa}$, respectively, and the valence-band parameters γ_i can be derived from the magnetic-field-induced splitting and energy shift of the exciton ground-state subcomponents on the basis of the theory as outlined for example in Ref. 2. Compared to Ref. 2 we will discuss our results in terms of $|m_j\rangle\alpha, |m_j\rangle\beta$ basis functions, which in the case of negligible electron-hole spin exchange are more appropriate than the $J=1$, $J=2$ basis. α, β are the usual spin functions characterizing conduction band states, the states of the Γ_8 valence band ($J=\frac{3}{2}$) are represented by $|m_j\rangle$, $m_j = \pm\frac{1}{2}, \pm\frac{3}{2}$.

For $\vec{B}\|[100]$ the energy separation between the $|\frac{3}{2}\rangle\beta$ and $|-\frac{3}{2}\rangle\alpha$ states, corresponding to the predominant transitions observable in Faraday configuration for σ^+ and σ^- polarization, are given by[2]

$$E(|-\tfrac{3}{2}\rangle\alpha) - E(|\tfrac{3}{2}\rangle\beta) = (6\tilde{\kappa} + g_c + \tfrac{27}{2}\tilde{q})\mu_B H = g_{\sigma,100}\mu_B H\,, \tag{3.9}$$

where μ_B is the Bohr magneton. The splitting between the $|\frac{1}{2}\rangle\beta$ and $|-\frac{1}{2}\rangle\alpha$ states, observable for π polarization in Voigt configuration, is given by[2]

$$E(|-\tfrac{1}{2}\rangle\alpha) - E(|\tfrac{1}{2}\rangle\beta) = (2\tilde{\kappa} + g_c + \tfrac{1}{2}\tilde{q})\mu_B H = g_{\pi,100}\mu_B H\,. \tag{3.10}$$

The diamagnetic shift rate $\Delta E_{\mathrm{dia},\sigma}$ of the $|\frac{3}{2}\rangle\beta$ and $|-\frac{3}{2}\rangle\alpha$ states and the shift $\Delta E_{\mathrm{dia},\pi}$ of the $|-\frac{1}{2}\rangle\alpha$ and $|\frac{1}{2}\rangle\beta$ states are given for $\vec{B}\|[100]$ by

$$\Delta E_{\mathrm{dia}}\begin{pmatrix}\sigma\\ \pi\end{pmatrix} = \tfrac{1}{2}\gamma^2 R_0(1 - \nu \pm \delta')\,, \tag{3.11}$$

where

$$\tilde{\kappa} = \kappa - d - \tfrac{13}{6}d(\tau - 1)\,, \tag{3.12a}$$

$$\tilde{q} = q + \tfrac{2}{3}d(\tau - 1)\,, \tag{3.12b}$$

$$d = \tfrac{32}{5}(\mu_0/m_0)\gamma_3^2 \times 0.281\,, \tag{3.12c}$$

$$\tau = \gamma_2/\gamma_3\,, \tag{3.12d}$$

$$1/\mu_0 = 1/m_e + \gamma_1/m_0\,, \tag{3.12e}$$

$$R_0 = \mu_0 e^4/2\hbar^2\epsilon_0^2\,, \tag{3.12f}$$

$$\gamma = e\hbar H/2\mu_0 c R_0\,, \tag{3.12g}$$

$$\nu = \tfrac{16}{15}(\mu_0\gamma_2/m_0)^2(2 + 3/\tau^2) \times 2.126\,, \tag{3.12h}$$

$$\delta' = 1.767\mu_0\gamma_2/m_0\,, \tag{3.12i}$$

and all other symbols have their usual meaning. k-linear contributions to $\tilde{\kappa}$ and $\tilde{q}$ have been neglected.

It should be noted, that $\Delta E_{\mathrm{dia},\sigma}$ in the present investigation is different from the expression given in Ref. 1, where the weighted average of the $|-\frac{3}{2}\rangle\alpha$, $|\frac{3}{2}\rangle\beta$ and $|-\frac{1}{2}\rangle\beta$, $|\frac{1}{2}\rangle\alpha$ state shift is considered. Secondly, as already pointed out in Ref. 2, the term in the exciton Hamiltonian giving rise to $16W/15$ (=0.767) in the expression for δ' in Ref. 2 is missing in Ref. 1. As a consequence the numerical factor 1.767 in Eq. (3.12i) is 1.0 in Ref. 1 only, and an analysis of experimental data on the basis of Ref. 1 would give a 77% larger value for γ_2 compared to the present results.

C. Polaron corrections

According to Eq. (3.11) the mean diamagnetic shift rate of the $|\frac{3}{2}\rangle\beta$, $|-\frac{3}{2}\rangle\alpha$, $|\frac{1}{2}\rangle\beta$, and $|-\frac{1}{2}\rangle\alpha$ states is mainly determined by the reduced exciton mass μ_0, and the difference of the shift for the $|\frac{3}{2}\rangle\beta$, $|-\frac{3}{2}\rangle\alpha$ states compared to that of the $|\frac{1}{2}\rangle\beta$, $|-\frac{1}{2}\rangle\alpha$ states is proportional to $\gamma_2\mu_0$. Thus γ_2 and μ_0 can be obtained from an analysis of experimentally determined diamagnetic shift rates. However, the validity of Eq. (3.11) is subject to the following restrictions: Eq. (3.11) is appropriate for (i) weak electron- (hole-exciton-) phonon interaction and (ii) low magnetic fields ($\gamma \ll 1$) only. In the present case $\gamma = 0.65$ at 18 T, and in addition ZnSe is a strongly polar material [$\epsilon_0 = 8.66$ (Ref. 17), $\epsilon_\infty = 5.9$ (Ref. 18)] with $r_{\mathrm{pol,el}} + r_{\mathrm{pol},h} \simeq a_0$, where $r_{\mathrm{pol},i}(i = \mathrm{el}, h)$ are the polaron radii of the electron and hole, and a_0 is the exciton Bohr radius. Consequently, in the present case simple application of Eq. (3.11) to the experimental data would yield incorrect results, since the diamagnetic shift rate is reduced, as γ becomes comparable to 1 (Refs. 19 and 20), and it is further reduced in polar materials.[4] Since no theory exists, which is really appropriate for the present case, i.e., valid for: (i) γ up to ~0.7, (ii) strong exciton-phonon interaction, and (iii) degenerate valence bands, we extended the validity range of the results given in Ref. 2 assuming that the diamagnetic shift rates for degenerate valence bands are reduced by the same amount as calculated according to Ref. 4 for an exciton in the corresponding two-band model. Then we get corrected diamagnetic shift rates

$$\Delta E_{\mathrm{dia}}^{\mathrm{corr}} = \Delta E_{\mathrm{dia}} F(\gamma)\,, \tag{3.13}$$

where $F(\gamma)$ is the result of the variational calculation. $F(\gamma)$ depends on m_e, γ_1, $\hbar\omega(LO)$, ϵ_0, and ϵ_∞. Apart from this correction the exciton-

(electron-, hole-) phonon interaction was taken into account regarding the parameters entering the analysis in Ref. 2 as renormalized parameters. Renormalized parameters are marked with an asterisk in contrast to the bare parameters without further label. The relation between renormalized and bare valence band parameters is given for example in Ref. 21.

IV. RESULTS

A. g factors

Reflectance spectra measured on a cleaved (110) face in Voigt configuration and π polarization for $\vec{B}\|[110]$ are shown in Fig. 1. (A zero magnetic field spectrum is shown in the upper part of Fig. 7). On the low-energy side of the main reflectance minimum an additional structure becomes observable at $B > 10$ T and transforms into a second reflectance minimum at higher fields. The two structures correspond to the $|\frac{1}{2}\rangle\beta$ and $|-\frac{1}{2}\rangle\alpha$ states. Best agreement between the calculated reflectance and the experimental results is obtained taking a zero-magnetic-field oscillator strength $4\pi\beta(B=0) = 6.5\times10^{-3}$, corresponding to a longitudinal-transverse (L-T) splitting of 1.1 meV (for a background dielectric constant at the exciton energy $\epsilon_b = 8.1$ (Refs. 18 and 22). Hite *et al.*[9] report $4\pi\beta = (5.5\pm0.7)\times10^{-3}$, obtained from normal incidence reflectance, Kramers-Kronig inversion to get the exciton absorption and subsequent integration. With increasing magnetic field the oscillator strength increases and for 18 T we calculate $4\pi\beta(18\text{ T}) = 7.8\times10^{-3}$ according to Ref. 19. The splitting between the two π states was linear over the whole range investigated and within experimental error the same for $\vec{B}\|[100]$ and $\vec{B}\|[110]$. The best fit to the experimental data is obtained assuming equal oscillator strength for both states for all spectra. Calculating the splitting of the two π states with a short-range electron-hole spin exchange energy $2\Delta_1 = 0.1$ meV [$-2\Delta_1$ is the energy separation between the $J=1$ (Γ_5) and the $J=2$ ($\Gamma_3+\Gamma_4$) state for $B=0$] we get oscillator strengths with relative intensities 2:3 at 12 T. Since larger deviations from equal relative oscillator strengths of the two π-polarized states would have been observable in our experiments we conclude

$$2\Delta_1 \lesssim 0.1 \text{ meV}. \tag{4.1}$$

Accordingly we neglected a possible influence of Δ_1 on the observed linear Zeeman splitting and then obtain

$$g_{\pi,100} = 2\bar{k} + g_c + \tfrac{1}{2}\bar{q} = 0.95\pm0.20. \tag{4.2}$$

The splitting between the predominant transi-

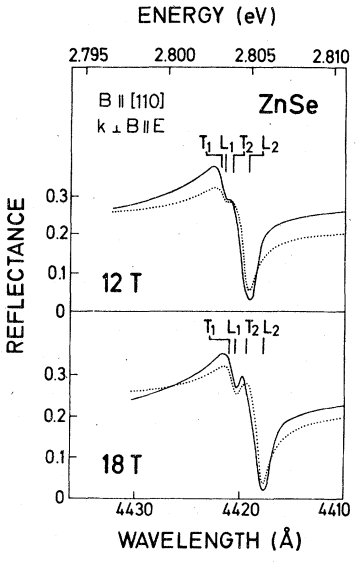

FIG. 1. Normal-incidence reflectance for two different magnetic field strengths (Voigt configuration, π polarization). Full lines: experimental spectra; dotted lines: theoretical results (exciton free layer: 40 Å; damping constant $\Gamma = 0.4$ meV, equal strength for both oscillators). T, L: energies of transverse and longitudinal exciton states. Absolute reflectance derived from fit to theoretical value for long wavelengths assuming $\epsilon_b = 8.1$ (Refs. 18 and 22).

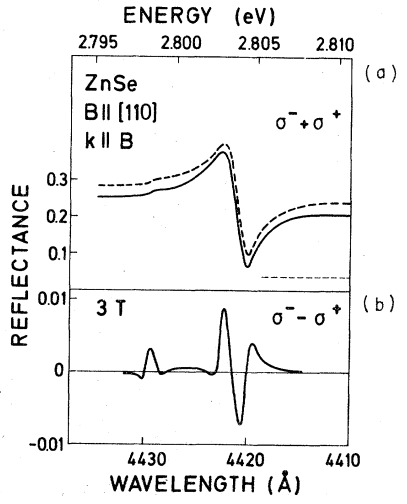

FIG. 2. (a) Sum of σ^+- and σ^--polarized reflectance at 3 T (full line). Broken line: reflectance for $B=0$. (b) Difference of σ^-- and σ^+-polarized reflectance at 3 T.

tions observable in Faraday configuration for σ^+ and σ^- polarization turned out to be small compared to the linewidth of the reflectance structure. For this reason the sum and the difference of the σ^+ and σ^- polarized reflectance were measured simultaneously and the g factor derived from these spectra. Even for low magnetic fields ($B \simeq 1$ T) the σ^+- and σ^--polarized spectra had different shapes in the energy region of the main reflectance maximum. The σ^+-reflectance maximum was lower than the σ^- maximum, and since the $|\frac{3}{2}\rangle\beta$ state is at higher energies than the $|-\frac{3}{2}\rangle\alpha$ state, the lineshape difference has the consequence for the observed difference spectrum that the main negative peak (at 2.804 eV in Fig. 2) appears reduced compared to the value expected in a rigid shift model. On the high energy side of the reflectance minimum we did not observe any indication of different lineshapes for σ^+- and σ^--polarized reflectance, but the difference spectrum had the same lineshape as the energy derivative of the direct spectrum. Thus we determined the energy splitting from this part of the spectrum and obtained

$$\Delta E/B = (0.20 \pm 0.04 \text{ meV})/10 \text{ T}, \quad \text{for } \vec{B} \| [100], \tag{4.3}$$

$$\Delta E/B = (0.17 \pm 0.04 \text{ meV})/10 \text{ T}, \quad \text{for } \vec{B} \| [110]. \tag{4.4}$$

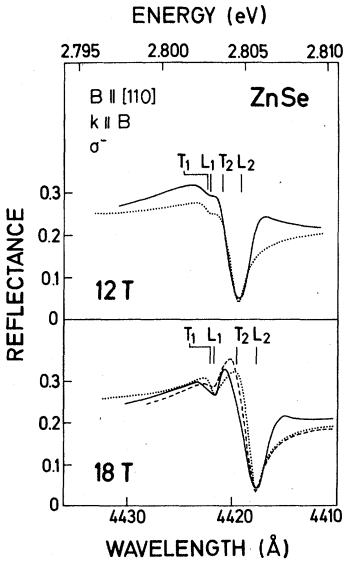

FIG. 3. Normal incidence reflectance for two different magnetic field strengths in Faraday configuration (σ^- polarization). Full and broken lines: experimental spectra for two samples, dotted lines: theoretical results (exciton free layer: 40 Å; damping constant $\Gamma = 0.4$ meV, 1:3 relative oscillator strengths).

For σ^- polarization a second reflectance structure is observed for $B > 12$ T, attributed to the $|-\frac{1}{2}\rangle\beta$ state (cf. Fig. 3), while the main reflectance structure is attributed to the $|-\frac{3}{2}\rangle\alpha$ state. Comparison between theoretical and experimental reflectance curves suggests an intensity ratio 1:3 for the two oscillators as expected for the case of negligible electron-hole spin exchange energy Δ_1 compared to the linear Zeeman splitting. For σ^+ polarization even at 18 T only a single reflectance structure could be observed as a consequence of a small energy difference between the $|\frac{3}{2}\rangle\beta$ and $|\frac{1}{2}\rangle\alpha$ states. Starting with an approximate value for g_c and $\tilde{\kappa}$, the energy position of the transverse $|\frac{3}{2}\rangle\beta$ state related to the observed reflectance minimum was calculated according to Ref. 5, yielding more accurate values for g_c and $\tilde{\kappa}$. Repeating this procedure two or three times one gets self-consistent results and thus we derive

$$g_{\sigma,100} = 6\tilde{\kappa} + g_c + \tfrac{27}{2}\tilde{q} = -0.13 \pm 0.08, \tag{4.5}$$

$$g_{\sigma,110} = -0.08 \pm 0.08. \tag{4.6}$$

The large energy separation between the $|-\frac{3}{2}\rangle\alpha$ and $|-\frac{1}{2}\rangle\beta$ states (σ^- polarization) compared to that between the $|\frac{3}{2}\rangle\beta$ and $|\frac{1}{2}\rangle\alpha$ states (σ^+ polarization) determines the sign of $g_{\pi,100}$ [Eq. (4.2)] by the following argument. The energy separation $\Delta E_{\sigma-(\sigma+)}$ between the two σ^- (σ^+) polarized states, respectively, is given by[2]

$$\Delta E_{\sigma-(\sigma+)} = (\pm 2\tilde{\kappa} \pm g_c + 2\delta' \pm \tfrac{13}{2}\tilde{q})\mu_B H, \tag{4.7}$$

where the upper (lower) sign corresponds to the $\sigma^-(\sigma^+)$-polarized states. Since δ' is always positive and the influence of $\frac{13}{2}\tilde{q}$ is significant, $2\tilde{\kappa} + g_c$ has to be positive.

From Eqs. (4.2), (4.5), and (4.6) the effective electron and hole g factors, g_c and $\tilde{\kappa}$, as well as the cubic parameter $\tilde{q}$ can be determined in principle. However, if the effective g factors $g_{\sigma,110}$ and $g_{\pi,110}$ are calculated from the complete exciton matrix and compared to the values $g_{\sigma,100}$ and $g_{\pi,100}$, respectively, the following result is obtained: If $\tilde{q}$ is chosen to give the calculated difference between $g_{\sigma,110}$ and $g_{\sigma,100}$ in accordance with the experimental results, one calculates a much larger difference between $g_{\pi,110}$ and $g_{\pi,100}$. On the other hand $g_{\pi,110} \simeq g_{\pi,100}$ implies $\tilde{q} \simeq 0$ which also yields $g_{\sigma,110} \simeq g_{\sigma,100}$. Due to the relatively large error of the experimentally determined g values we do not attribute significance to this discrepancy and choose $\tilde{q}$ as to obtain best overall agreement. Assuming $\tilde{q} = -0.02$ we get

$$\tilde{\kappa} = -0.21 \pm 0.06 \quad \text{and} \quad g_c = 1.37 \pm 0.25. \tag{4.8}$$

TABLE I. Fundamental parameters of cubic ZnSe.

Present experiments	Other results
$\gamma_1^* = 4.3 \pm 0.5$	4.32 [a]
$\gamma_2^* = 0.59 \pm 0.07$	0.66 [a]
$\gamma_3^* = 1.34 \pm 0.30$	1.13 [a]
$\gamma_1 = 4.8 \pm 0.6$	3.77 [b]
$\gamma_2 = 0.67 \pm 0.08$	1.24 [b]
$\gamma_3 = 1.53 \pm 0.35$	1.67 [b]
$\tilde{\kappa} = -0.21 \pm 0.06$	−0.14 [a]
$\kappa = -0.28 \pm 0.08$	
$g_c = 1.37 \pm 0.25$	1.18 [c]
	1.2 [a]
	1.46 [d]
	1.59 [e]
$m_e^*/m_0 =$ ...	0.16 [f]
$\mu_0^*/m_0 = 0.095 \pm 0.002$	0.105 [g]
	0.13 [h]
	0.098 [a]
$R_0^* = 16.8 \pm 0.4$ meV	19.9 meV [i]
$E_{1s} = 17.4 \pm 0.4$ meV	21 meV [j]
	18 meV [k]
$\epsilon_{\text{eff}} = 8.77$	$\epsilon_0 = 8.66$ [g]
	9.1 (at 300 K) [l]

[a] Reference 6.
[b] Reference 29.
[c] Reference 30.
[d] Reference 27.
[e] Reference 28.
[f] Reference 24.
[g] Reference 17.
[h] Reference 39.
[i] Reference 35.
[j] Reference 9.
[k] Reference 38.
[l] Reference 37.

Calculating $g_{\sigma,110}$ and $g_{\pi,110}$ with these parameters [Eq. (4.8)] from the complete exciton matrix we get $g_{\sigma,110} = -0.10$ and $g_{\pi,110} = 0.86$, valid as long as diamagnetic terms and off-diagonal mixing are negligible ($B < 5$ T in the present case).

B. Rydberg energy, reduced exciton mass, and valence-band parameters

Determination of the Rydberg energy R_0^* and of the valence band parameters γ_i cannot be done for a single quantity completely independent from the other parameters, since the experimentally observed energy separations and energy shifts are always dependent on all of these quantities. Thus after derivation of a complete set of parameters the analysis has to be redone until self-consistency is achieved. Evaluation of any quantity in the following has to be understood in this sense.

We observed an energy difference of 12.0 ± 0.3 meV between the 1s and 2s exciton reflectance minima, corresponding to (13.0 ± 0.3)-meV energy separation between the 1s and 2s transverse exciton states for 1.1-meV L-T splitting (cf. Sec. IV A). According to Ref. 23 this energy separation corresponds to $0.773 R_0^*$ for $\mu = 0.20$ (cf. Table I, definition of μ see Ref. 23, for example) and thus we get for the exciton Rydberg R_0^* and the exciton binding energy E_{1s}

$$R_0^* = 16.8 \pm 0.4 \text{ meV} \quad \text{and} \quad E_{1s} = 17.4 \pm 0.4 \text{ meV}. \tag{4.9}$$

Combining the exciton binding energy E_{1s} with the energy E_T of the transverse 1s exciton state ($E_T = 2.8027$ eV, cf. Ref. 7) we get the energy E_{gap} of the direct energy gap

$$E_{\text{gap}} = 2.8201 \pm 0.0004 \text{ eV}, \tag{4.10}$$

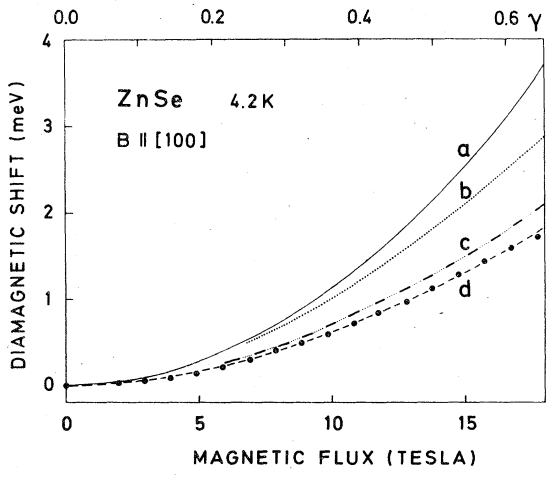

FIG. 4. Experimentally observed diamagnetic shift $\frac{1}{2}(\Delta E_{\text{dia},\sigma} + \Delta E_{\text{dia},\pi})$ (•) and theoretical curves for different models. (a) low-field hydrogenic formula $\Delta E = \frac{1}{2}\gamma^2 R_0^*$, (b) variational calculation (Refs. 4 and 19) neglecting polaron effects, (c) variational calculation (Ref. 4) including polaron effects for two-band model, (d) as (c), but reduced by factor $(1-\nu)$ for valence band degeneracy. Parameters used for calculation: $m_e^*/m_0 = 0.16$, $m_h^*/m_0 = 0.23$, $\epsilon_0 = 8.66$, $\epsilon_\infty = 5.9$, $\hbar\omega(\text{LO}) = 31$ meV. References see text.

at 1.6 K.

The experimentally determined diamagnetic shift 0.5 $(\Delta E_{\mathrm{dia},\sigma}+\Delta E_{\mathrm{dia},\pi})$ is given by the circles in Fig. 4. For π polarization and $B<10$ T only a single reflectance structure corresponding to the higher energy state $|-\frac{1}{2}\rangle\alpha$ was observed, and $\Delta E_{\mathrm{dia},\pi}$ was determined by

$$\Delta E_{\mathrm{dia},\pi}=E(|-\tfrac{1}{2}\rangle\alpha)-\tfrac{1}{2}g_{\pi}\mu_B H\,. \tag{4.11}$$

In order to obtain for a given electron effective mass m_e^* the exciton reduced mass μ_0^* the diamagnetic shift was calculated for an exciton in a two-band model[4] for $m_e^*/m_0=0.16$ (Ref. 24) and different values of the hole mass m_h^*. The final choice for m_h^* results from the curve giving best agreement with experiment after multiplication of the variational result by the factor $(1-\nu)$, i.e., correcting for the valence band degeneracy (cf. Sec. III C). From the results as shown in Fig. 4 we derive $m_h^*/m_0=0.23$, which corresponds to

$$\gamma_1^*=4.3\pm0.5\,, \tag{4.12}$$

on the basis of our theoretical model. The corresponding exciton reduced (polaron) mass is

$$\mu_0^*/m_0=0.095\pm0.003\,, \tag{4.13}$$

calculated according to Eq. (3.12e). The value for γ_2^* is derived from

$$(\Delta E_{\mathrm{dia},\sigma}-\Delta E_{\mathrm{dia},\pi})/(\Delta E_{\mathrm{dia},\sigma}+\Delta E_{\mathrm{dia},\pi})=\delta'/(1-\nu)=0.12\pm0.02\,. \tag{4.14}$$

According to Eqs. (3.12h) and (3.12i) we obtain

$$\gamma_2^*=0.59\pm0.07\,, \tag{4.15}$$

using the results (4.9) and (4.13).

If γ_2^* is known, γ_3^* can be derived from the splitting of the $|-\frac{1}{2}\rangle\beta$ and $|-\frac{3}{2}\rangle\alpha$ states for $\vec{B}\|[110]$. However, due to the mixing between the $|\frac{1}{2}\rangle$ and $|-\frac{3}{2}\rangle$ valence-band states and that between the $|-\frac{1}{2}\rangle$ and $|\frac{3}{2}\rangle$ states no simple expression for the splitting between the $|-\frac{1}{2}\rangle\beta$ and $|-\frac{3}{2}\rangle\alpha$ exciton states can be given for $\vec{B}\|[110]$, but one has to calculate the energy separation by diagonalizing the appropriate 2×2 matrix for different values of γ_3^*. We did this calculation only as a check for our valence band parameters, but derived γ_3^* from[25]

$$\kappa=\gamma_3+\tfrac{2}{3}\gamma_2-\tfrac{1}{3}\gamma_1-\tfrac{2}{3}\,, \tag{4.16}$$

κ is obtained from Eqs. (3.12a) and (4.8). According to Ref. 21 and using $\epsilon_0=8.66$ (Ref. 17), $\epsilon_\infty=5.9$ (Ref. 18), and $\hbar\omega(\mathrm{LO})=31$ meV (Ref. 26) we calculate

$$\gamma_1/\gamma_1^*=1.12\,,\quad \mu/\mu^*=1.02\,,$$
$$\text{and } \gamma_2/\gamma_2^*=\gamma_3/\gamma_3^*=1.14\,, \tag{4.17}$$

where we assumed the same relative change for γ_2 and γ_3 due to renormalization of the bare valence band parameters. Eqs. (4.16) and (3.12a) yield a quadratic equation for the determination of γ_3^*, and with Eqs. (4.8), (4.12), (4.13), (4.15), and (4.17) we derive

$$\gamma_3^*=1.34\pm0.30\,. \tag{4.18}$$

In order to test the reliability of the parameters γ_2^* and γ_3^* derived we checked the consistency with the experimental results not used for the analysis and calculated the energy shift of all six dipole allowed exciton substates for $\vec{B}\|[100]$ and $\vec{B}\|[110]$. The parameters used for the calculation are those compiled in Table I. Theoretical curves and the experimental data for $\vec{B}\|[110]$ and σ^+, σ^- and for π polarization are shown in Figs. 5 and 6. The weak $|\frac{1}{2}\rangle\alpha$ state giving rise to a σ^+-polarized transition could not be observed experimentally as a consequence of the small energy separation to the $|\frac{3}{2}\rangle\beta$ state. The energy of the $|-\frac{1}{2}\rangle\beta$ state depends (in addition to $\bar{\kappa}$ and g_c) on γ_2^* and γ_3^*, and the good agreement between experiment and theory is interpreted as a confirmation of the values for γ_2^* and γ_3^* derived, since the energy of

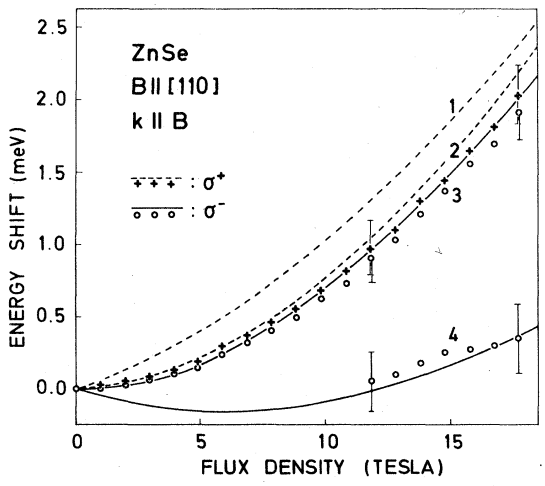

FIG. 5. Calculated energy shift of $|\frac{1}{2}\rangle\alpha$ (curve 1), $|\frac{3}{2}\rangle\beta$ (curve 2), $|-\frac{3}{2}\rangle\alpha$ (curve 3), and $|-\frac{1}{2}\rangle\beta$ state (curve 4) for $\vec{B}\,||\,[110]$ from the complete exciton matrix (Ref. 2) modified according to Eq. (3.13). Parameters for the calculation are given in Table I. Experimental results: +, o

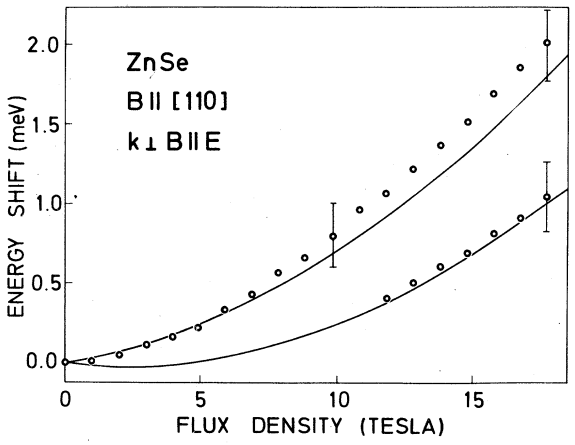

FIG. 6. Calculated energy shift of $|-\frac{1}{2}\rangle\,\alpha$ (upper curve) and $|\frac{1}{2}\rangle\,\beta$ (lower curve) for $\vec{B}$ ∥ [110] from the complete exciton matrix (Ref. 2) modified according to Eq. (3.13). Parameters for the calculation are given in Table I. Experimental results: o

the $|-\frac{1}{2}\rangle\beta$ state was not considered for the evaluation of any parameter.

For $\vec{B}\|[100]$ the calculated energy separation between the $|-\frac{1}{2}\rangle\beta$ and $|-\frac{3}{2}\rangle\alpha$ states is 1.27 meV at 18 T, while we observed only 1.0 ± 0.3 meV. The agreement between the calculated energy separation and the experimental results is considered satisfactory taking into account that the low-energy reflectance structure was much less pronounced for $\vec{B}\|[100]$ than for $\vec{B}\|[110]$, thus introducing a relatively large experimental error, and secondly that our theoretical model is a first approximation only.

V. DISCUSSION

The conduction-band electron g factor determined in the present experiments is in agreement with existing theoretical $(\vec{k}\cdot\vec{p})$ calculations. Cardona[27] calculated $g_c = 1.46$ assuming the same interband matrix element $E_p = 21$ eV for all II-VI compounds and using wave functions of the isoelectronic nonpolar material by application of an antisymmetric perturbing potential. Bowers and Mahan[28] calculated $g_c = 1.59$ using pseudo wave functions and considering interactions between the valence band and the first conduction band. Lawaetz[29] did a five-level $\vec{k}\cdot\vec{p}$ analysis and derived momentum matrix elements in a semiempirical way as a function of lattice constant, ionicity and d-electron contributions. The g value $g_c = -5.74$ is apparently wrong due to an algebraic error, and taking the expression for the g factor and the parameters given in Ref. 29 one gets $g_c = 0.92$, somewhat lower than our experimental result.

Fleury and Scott[30] derived $g_c = 1.18$ from spin-flip Raman scattering on In-doped ZnSe, and Feierabend and Weber[6] obtained recently $g_c = 1.2$. This latter value was derived from the experimentally observed splitting between the predominant σ^+- and σ^--polarized transitions in magnetoreflectance combined with the effective g factor for Voigt configuration and π polarization determined by Venghaus and Lambrich.[7] The discrepancy with $g_c = 1.37$ derived in the present investigation is due to the fact, that Feierabend and Weber assumed a short-range electron-hole spin exchange energy $2\Delta_1 = 0.3$ meV in contrast to our result $2\Delta_1 \lesssim 0.1$ meV [cf. Eq. (4.1)].

Our result $2\Delta_1 \lesssim 0.1$ meV differs also from $2\Delta_1 = 1.0$ meV derived by Langer *et al.*,[31] however, the large value for $2\Delta_1$ in Ref. 31 is attributed to an incorrect analysis of the experimental data, since it is based on the relative separation of reflectance minima. Our result for Δ_1 is also in disagreement with a theoretical value $2\Delta_1 = 1.25$ meV,[32] but this fairly large value has already been interpreted as an artifact of the calculation based on nonorthogonal plane waves.[33] On the other hand, our present result is in qualitative agreement with the value derived for ZnTe from uniaxial stress measurements ($\Delta_1 \lesssim 0.01$ meV),[34] and comparable results for ZnTe and ZnSe correspond to what one would expect.

The exciton Rydberg R_0^* and binding energy E_{1s} determined in the present investigation are somewhat small compared to most other results published earlier. Sondergeld and Stafford[35] derived $R_0 = 19.9$ meV from the $2P$-$3P$ exciton-state separation measured by two-photon absorption. Details of the analysis are not given. Aven *et al.*[22] obtained (20 ± 4)-meV exciton binding energy from reflectance data. Fujiwara *et al.*[36] performed electroreflectance measurements and estimated the exciton binding energy to be 22.9 meV, using the room temperature dielectric constant $\epsilon_0 = 9.1$ (Ref. 37) and an exciton reduced mass $\mu_0 = 0.15m_0$, which is definitely too large compared to $m_e^* = 0.16m_0$ (Ref. 24). Hite *et al.*[9] report 21-meV exciton binding energy from normal incidence reflectance and subsequent Kramers-Kronig analysis. Their original data show 12.6-meV energy separation between the $n = 1$ and $n = 2$ exciton state reflectance minima and are in good agreement with the present experiments, but in contrast to their final result. Accordingly we

attribute the discrepancy for the binding energy to their method of analysis. Finally, Röppischer *et al.*[38] obtained 18-meV exciton binding energy from reflectance measurements in good agreement with our own results.

Our result for the exciton reduced mass [Eq. (4.13)] compares favorably with $\mu_0 = 0.098 \pm 0.002$ derived by Feierabend and Weber[6] from magnetoreflectance, and also with $\mu_0 = 0.10 \pm 0.03$ given by Aven *et al.*[22] Mass values given by other authors are in general slightly larger corresponding to their larger Rydberg. Segall and Marple[17] report $\mu_0 = 0.105$ and Riccius and Turner[39] even $\mu_0 = 0.13 \pm 0.01$.

A consistency check for R_0^* and μ_0^*, which we derived from two independent measurements, is given by the hydrogenic formula [Eq. (3.12f)]. From μ_0^* and using $\epsilon_0 = 8.66$ (Ref. 17) we calculate $R_0^* = 17.2$ meV close to our experimental results for R_0^*. Taking alternatively our results for μ_0^* and R_0^* we derive an effective dielectric constant $\epsilon_{\text{eff}} = 8.77$ in close agreement with $\epsilon_0 = 8.66$ (Ref. 17).

The valence-band parameters γ_i derived here differ significantly from a previous analysis of the data ($\gamma_1 = 2.17$, $\gamma_2 = 0.63$, $\gamma_3 = 0.97$),[40] where the reduction of the diamagnetic shift in polar materials[4] had not been considered and polaron effects were taken into account by mass renormalization only.

Valence-band parameters obtained by Lawaetz[29] in a $\vec{k} \cdot \vec{p}$ calculation deviate considerably from our results as far as γ_1 and γ_2 are concerned, while γ_3 is in good agreement. Trebin developed a theoretical model for excitons in polar materials[41] and combined his results with the splitting of the $2P$ exciton states determined by two-photon absorption.[42] Using $R_0 = 19.9$ meV and $m_e^* = 0.18 m_0$ Trebin derived a set of valence band parameters $\gamma_1 = 3.2$, $\gamma_2 = 0.58$, $\gamma_3 = 1.00$. The agreement with our results is poor, but the difference will decrease, if a smaller R_0 as suggested by our experiments and $m_e^* = 0.16 m_0$ (Ref. 24) are taken for the analysis.

The energy separation of $2P$ exciton states does not only represent a means to determine valence band parameters, as has been done by Sondergeld,[42] but also provides the possibility to test parameters derived from other data. According to Ref. 23 and using the renormalized parameters given in Table I we calculate the following $2P$ state energies: $E(2P_{1/2}) = 3.49$ (3.39) meV, $E[2P_{5/2}(\Gamma_7)] = 3.94$ (4.0) meV, $E[2P_{5/2}(\Gamma_8)] = 4.34$ (4.35) meV, and $E(2P_{3/2}) = 5.13$ (5.10) meV. Sondergeld's experimental data[42] are given in parentheses, and since only relative positions of the $2P$ states were measured, the original data have been reduced by 0.8 meV for convenience in comparison. The agreement between our calculated and the experimentally determined energies is very close and represents a good confirmation of the reliability of our data.

VI. EXCITED EXCITON STATES

In addition to the exciton ground state we investigated the magnetic field dependence of excited exciton states. Reflectance curves were obtained by integration of the originally measured wavelength derivative spectra. Results are shown in Fig. 7, the energy shift of the structures observed for σ^+, σ^-, and π polarization (for Faraday and Voigt configuration, respectively), are given in Fig. 8.

An adequate theoretical model to describe our experiments does not exist at present. Swierkow-

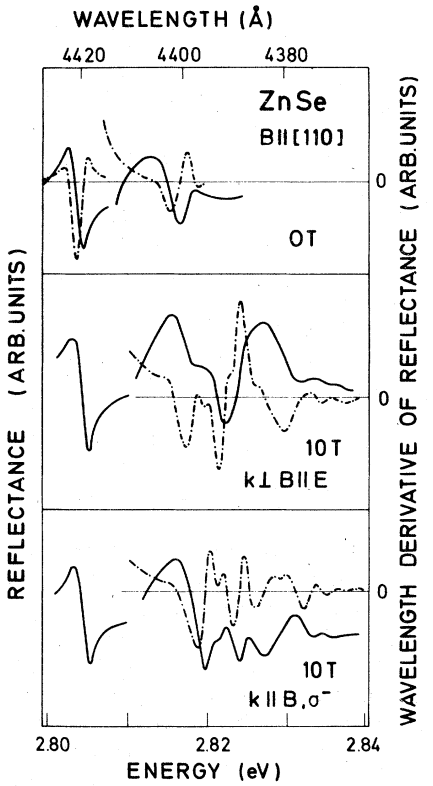

FIG. 7. Wavelength derivative of normal incidence reflectance (dashed-dotted curves) and reflectance obtained by integration (solid lines) for different magnetic fields and configurations. $1s$ ground state and excited state related structures are given in different scales, zero of direct reflectance omitted.

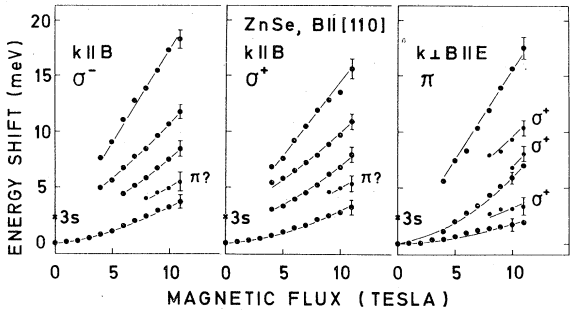

FIG. 8. Energy shift of excited exciton states (reflectance minima plotted). Zero energy corresponds to position of 2s state for $B=0$. "3s" indicates calculated energy of 3s state. Curves plotted as guidelines to the eye. $\sigma^{\pm}(\pi)$ in the $\pi(\sigma^{\pm})$ spectra indicates coincidence with strong structure observed in $\sigma^{\pm}(\pi)$ spectrum.

ski[43] did not consider 2P states and calculated 2S state energies for $\gamma \ll 1$ only. Under the present circumstances, however, the corrections to the hydrogenic diamagnetic shift rate due to the band structure are much smaller than the overall reduction of the diamagnetic shift of a hydrogenic 2S state.[19,20] On the other hand, calculation of the excited states of a hydrogenic atom in a magnetic field[20] yields a simplified picture, since band structure effects are neglected, in contrast to the observation, that already at zero magnetic field the envelope-hole coupling splits the 2P exciton state into four substrates having energy separations of the order of 1 meV.[42] Finally, even 11 T is far below the lower-field limit of high-field theories,[44] thus these are not appropriate either.

In addition to the fact, that existing calculations[20] can serve as a guideline only for the interpretation of our results, an additional uncertainty arises from the impossibility to trace most of the states observable at higher magnetic field down to $B=0$, which would help to identify the observed structures (as $n=2$, $n=3$, etc., state related).

On the basis of the g factors derived from the 1S exciton states we estimate linear Zeeman effects to be small compared to the observed line separations. Consequently different structures are interpreted as different orbital states and not as Zeeman multiplets. Attributing the predominant structure for any given polarization to the 2S state, the additional structures may be related to higher S (and D states, which mix with the S states) or to 2P states. Selection rules for transitions to these states can be calculated according to Refs. 45 and 46. Considering only spin-singlet combinations of the Bloch functions, since these are expected to be predominant, the result is: Transitions to envelope states having $m_j = \pm 1$ are prevailing for π polarization, while σ^+, σ^--polarized states are related to $m_j = 0$.

Then we are able to give the following interpretation: The states observed for σ^+ and σ^- polarization are in principle the same, the differences are due to the different band-to-band transitions involved. According to Lee *et al.*[47] the even parity states next highest to 2S are the 3D and 3S states, where the relative oscillator strengths of these three states are 1 : 0.5 : 0.2 for $\gamma = 0.3$. Accordingly we interpret the three lowest σ^+- and σ^--polarized states as 2S, 3D, and 3S. The highest energy structure exhibits an energy shift close to that given by $1.5\hbar\omega_c = 1.5e\hbar H/c\mu_0^*$, which is 18.3 meV at 10 T, and since states having $m_j = +1$ cluster below the $N=1$ Landau level[47] the highest energy structure for σ^+ and σ^- polarization are interpreted as $2P(m_j = +1)$ related.

For Voigt configuration and π polarization the strongest transition is again expected to correspond to the 2S state. As can be seen from Fig. 7, there are two states of comparable intensity at low energies, the strongest being the higher-energy component. (A relative intensity reduction of the lower-energy state due to interaction with the higher-energy oscillator is negligible, since the energy separation is large compared to the L-T splitting. The structures appear broad due to large damping only, but not due to large oscillator strength.) Thus attributing the strongest structure to the 2S state, the other transition having the smallest shift rate is most likely to correspond to the $2P(-1)$ state, and the highest energy structure is attributed to the $2P(+1)$ state. The additional weak structures coincide with strong σ^+-polarized states and are consequently attributed to the corresponding transitions. Making these assignments the shift rate of the 2S state is larger in Voigt configuration for π polarization than for σ^+ and σ^- polarization in Faraday configuration. This is different from the situation in the low-field limit[43] and might be taken as an argument to interpret the lowest-energy π state as 2S and leaving the strongest structure unidentified. We do not favor this alternative, but a definite conclusion concerning this particular point cannot be given at present.

VII. CONCLUSIONS

Reflectance spectra were measured on cubic ZnSe crystals in magnetic fields up to 18 T and transverse energies of the 1s exciton states derived by line-shape analysis. In order to characterize the exciton states and to derive fundamental parameters, we combined the existing low field theory of Γ_6-Γ_8 exciton states[2] with the results of variational calculations for excitons in polar materials without valence band degeneracy.[4] We thus obtained a theoretical model applicable (i) to polar materials such as ZnSe and (ii) beyond the limit $\gamma \ll 1$.

Our experiments yield values for the electron and hole effective g factor, the exciton reduced mass, the exciton Rydberg and a set of valence-band parameters γ_i (cf. Table I). A consistency and reliability check for the parameters derived and a justification for the theoretical model applied is provided by the following facts: (i) Using the parameters obtained, energy shifts and splittings of exciton states not used for the evaluation of the parameters are calculated in good agreement with the experimental results. (ii) The exciton reduced mass derived from diamagnetic shift rates yields an exciton Rydberg in good agreement with the Rydberg calculated from the measured 1s-2s exciton state energy separation. (iii) The energy separations of 2P exciton states calculated from our parameters are in close agreement with two-photon absorption measurements.

The results of the present investigation suggest to derive fundamental parameters of related compounds such as CdTe or ZnTe along the lines of this paper. In the case of ZnTe these parameters are of particular current interest for a comparison between calculated and experimentally observed acceptor states.[48] In the case of CdTe, however, some additional difficulty is expected, since the k-linear term cannot be neglected[49] in contrast to the present case.

ACKNOWLEDGMENTS

The author is indebted to L. Greene from Wright-Patterson Air Force Base, Dayton, Ohio, for supplying the ZnSe boule from which the samples were cleaved and cut; to the members of the Max-Planck-Institut für Festkörperforschung in the high magnetic field laboratory (Grenoble) for their hospitality; to R. Lambrich for cooperation in part of the experiments; to H. G. Fischer, H. Hirt, and P. Wurster for expert technical assistance; to G. Behnke for performing the variational calculation of the exciton shift in polar materials; to J. Lagois and K. Cho for making available computer programs for the calculation of reflectance curves and exciton splittings in magnetic fields; and to U. Rössler for many helpful discussions.

[1] M. Altarelli and N. O. Lipari, Phys. Rev. B 7, 3798 (1973).
[2] K. Cho, S. Suga, W. Dreybrodt, and F. Willmann, Phys. Rev. B 11, 1512 (1975); 12, 1608 (1975).
[3] D. Bimberg, in *Advances in Solid State Physics*, edited by J. Treusch (Vieweg/Pergamon, Braunschweig, 1977), Vol. XVII, p. 195.
[4] G. Behnke, H. Büttner, and J. Pollmann, Solid State Commun. 20, 873 (1976).
[5] J. Lagois, Phys. Rev. B 16, 1699 (1977).
[6] S. Feierabend and H. G. Weber, Solid State Commun. 26, 191 (1978).
[7] H. Venghaus and R. Lambrich, Solid State Commun. 25, 109 (1978).
[8] T. Ichimiya, T. Niimi, K. Mizuma, O. Mikami, Y. Kamia, and K. Ono, in *Solid State Physics in Electronics and Telecommunications* (Academic, New York, 1960), p. 845.
[9] G. E. Hite, D. T. F. Marple, M. Aven, and B. Segall, Phys. Rev. 156, 850 (1967).
[10] D. D. Sell, S. E. Stokowski, R. Dingle, and J. V. DiLorenzo, Phys. Rev. B 7, 4568 (1973).
[11] E. O. Kane, Phys. Rev. B 11, 3850 (1975).
[12] S. I. Pekar, Sov. Phys. JETP 6, 785 (1958); Sov. Phys. Solid State 4, 953 (1962).
[13] J. J. Hopfield and D. G. Thomas, Phys. Rev. 132, 563 (1963).
[14] T. Skettrup and I. Balslev, Phys. Rev. B 3, 1457 (1971).
[15] H. Wolter, in *Handbuch der Physik*, edited by S. Flügge (Springer, Berlin, 1956), Vol. XXIV, p. 461.
[16] K. Lösch, thesis (University of Stuttgart, Germany, 1977) (unpublished).
[17] B. Segall and D. T. F. Marple, in *Physics and Chemistry of II-VI Compounds*, edited by M. Aven and J. S. Prener (North-Holland, Amsterdam, 1967), p. 319.
[18] D. T. F. Marple, J. Appl. Phys. 35, 539 (1964).
[19] D. Cabib, E. Fabri, and G. Fiorio, Nuovo Cimento B 10, 185 (1972).
[20] H. C. Praddaude, Phys. Rev. A 6, 1321 (1972).
[21] H. R. Trebin and U. Rössler, Phys. Status Solidi B 70, 717 (1975); H. R. Trebin, *ibid.* B 81, 527 (1977).
[22] M. Aven, D. T. F. Marple, and B. Segall, J. Appl. Phys. 32, 2261 (1961).
[23] A. Baldereschi and N. O. Lipari, Phys. Rev. B 8, 2697 (1973); B 9, 1525 (1974).
[24] J. L. Merz, H. Kukimoto, K. Nassau, and J. W. Shiever, Phys. Rev. B 6, 545 (1972).
[25] C. R. Pidgeon and R. N. Brown, Phys. Rev. 146, 575 (1966).
[26] J. C. Irwin and J. LaCombe, Can. J. Phys. 48, 2499

(1970); J. L. LaCombe and J. C. Irwin, Solid State Commun. 8, 1427 (1970).
[27]M. Cardona, J. Phys. Chem. Solids 24, 1543 (1963); 26, 1351 (1965).
[28]R. L. Bowers and G. D. Mahan, Phys. Rev. 185, 1073 (1969).
[29]P. Lawaetz, Phys. Rev. B 4, 3460 (1971).
[30]P. A. Fleury and J. F. Scott, Phys. Rev. B 3, 1979 (1971).
[31]D. W. Langer, R. N. Euwema, K. Era, and T. Koda, Phys. Rev. B 2, 4005 (1970).
[32]P. G. Rohner, Phys. Rev. B 3, 433 (1971).
[33]O. Schütz and J. Treusch, Solid State Commun. 13, 1155 (1973).
[34]W. Wardzyński, W. Giriat, H. Szymczak, and R. Kowalczyk, Phys. Status Solidi B 49, 71 (1972).
[35]M. Sondergeld and R. G. Stafford, Phys. Rev. Lett. 35, 1529 (1975).
[36]S. Fujiwara, K. Hattori, and M. Fukai, Phys. Lett. A 31, 258 (1970).
[37]D. Berlincourt, H. Jaffe, and L. R. Shiozawa, Phys. Rev. 129, 1009 (1963).
[38]G. Röppischer, I. Jacobs, and B. V. Novikov, Fiz. Tverd. Tela 17, 2178 (1975) [Sov. Phys. Solid State 17, 1442 (1976)].
[39]H. D. Riccius and R. Turner, J. Phys. Chem. Solids 28, 1623 (1967).
[40]H. Venghaus, Solid State Commun. 26, 199 (1978).
[41]H. R. Trebin, thesis (University of Regensburg, Germany, 1976) (unpublished).
[42]M. Sondergeld, Phys. Status Solidi B 81, 253 (1977); 81, 451 (1977).
[43]L. Świerkowski, Nuovo Cimento B 29, 340 (1975).
[44]M. Altarelli and N. O. Lipari, Phys. Rev. B 9, 1733 (1974).
[45]K. Cho, Phys. Rev. B 14, 4463 (1976).
[46]G. F. Koster, J. O. Dimmock, R. G. Wheeler, and H. Statz, *Properties of the Thirty-Two Point Groups* (M.I.T., Cambridge, Mass., 1963).
[47]N. Lee, D. M. Larsen, and B. Lax, J. Phys. Chem. Solids 34, 1059 (1973).
[48]D. C. Herbert, P. J. Dean, H. Venghaus, and J. C. Pfister, J. Phys. C 11, 3641 (1978); H. Venghaus, P. J. Dean, P. E. Simmonds, and J. C. Pfister, Z. Phys. B 30, 125 (1978).
[49]K. Cho, W. Dreybrodt, P. Hiesinger, S. Suga, and F. Willmann, *Proceedings of the Twelfth International Conference on the Physics of Semiconductors, Stuttgart, 1974*, edited by M. H. Pilkuhn (Teubner, Stuttgart, 1974), p. 945.